REPORT TO DAMES & MOORE

SEISMIC ANALYSIS OF THE METTER FEED HOLD TANK (MFHT)

Subconsultant: Medhat A. Haroun, Ph.D., P.E.
Professor and Chairman

Al Zeiny, Ph.D. Candidate

Hussain Bhatia, Ph.D. Candidate

Dept. of Civil and Environmental Eng.
University of California at Irvine

August 1995

1 Introduction

Under earthquake excitations, the overturning moment exerted by the hydrodynamic pressures on the unanchored Metter Feed Hold Tank (MFHT) tends to lift the shell off the floor, thus resulting in a nonlinear uplift problem. As shown in Figure (1), additional complexities involved in the analysis of this tank are due to large deformation of the base plate, floor-tank interaction and free-surface liquid-sloshing. A nonlinear finite element program DYNAZ [2] was used as the primary tool in solving the tank-floor problem under static and dynamic load conditions.

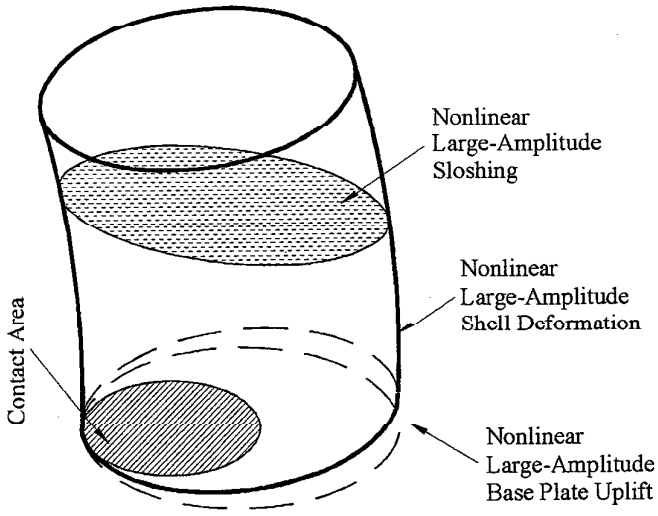

Figure 1: Complexities Associated with the Analysis of Unanchored Tanks

2 Tank Dimensions and Properties

The main properties and dimensions of the analyzed tank are:

Diameter ($D = 2R$) = 10 ft;
Height of fluid (H) = 8.42 ft;
Freeboard = 1.6 ft;
Thickness of bottom plate = 0.75 in;
Shell wall thickness (constant) = 0.5 in;
Roof thickness = 0.875 in;
Yield stress = 30,000 ksi;
E = 30×10^6 psi; and
Liquid and steel specific gravity = 1.5 and 7.85, respectively.

3 DYNAZ Program Description

The DYNAZ program is a three-dimensional finite element based computer program capable of simulating the complex dynamic behavior of various types of liquid storage tanks when subjected to strong seismic base excitations. The program takes into consideration contact, material, geometric nonlinearities as well as both the large amplitude liquid sloshing and the nonlinear fluid-structure interaction. The program has the following features:

- An up-to-date finite element technology in the analysis of solids and curved shells using the degeneration concept considering both material plasticity and geometric nonlinearity. Material plasticity is accounted for in various ways. The program is expandable to accommodate any desired new plastic model.
- Potential flow modeling through the usage of an efficient Eulerian formulation.
- Free surface sloshing modeling which utilizes the nonlinear wave theory formulation. The updated Lagrangian description of the fluid domain boundaries is utilized to keep track of the free surface position at any time.
- A variational principle that forms the basis for the numerical discretization of nonlinear fully coupled fluid-structure interaction problems with free surface sloshing. Since a Lagrangian description of the solid motion is utilized, the program uses an updated Eulerian-Lagrangian description of the fluid-solid interface in order to enforce compatibility between solid and fluid elements. The resulting nonlinear Euler-Lagrange equations are solved using an efficient time integration technique that has been developed especially to solve fluid-structure interaction problems.
- General contact analysis which accommodates a wide range of contact problems including fluid-structure interaction problems. A Lagrange multiplier technique was employed to enforce both displacement compatibility and force transmissibility constraints along the unknown contact surface. The program handles efficiently the special contact case of unanchored liquid storage tanks.

4 Static Analysis

A static analysis was performed to investigate the tank stability against buckling and against overturning. As shown in Figure (2), a hydrodynamic pressure distribution was assumed on the tank wall as

$$p = p_o \left(1 - \frac{y^2}{H^2}\right) \cos\theta$$

where y is the elevation of a point on the shell measured from the base, H is the fluid depth, θ is the angle measured from the axis of excitation and p_o is the pressure amplitude at the tank base at $\theta = 0°$.

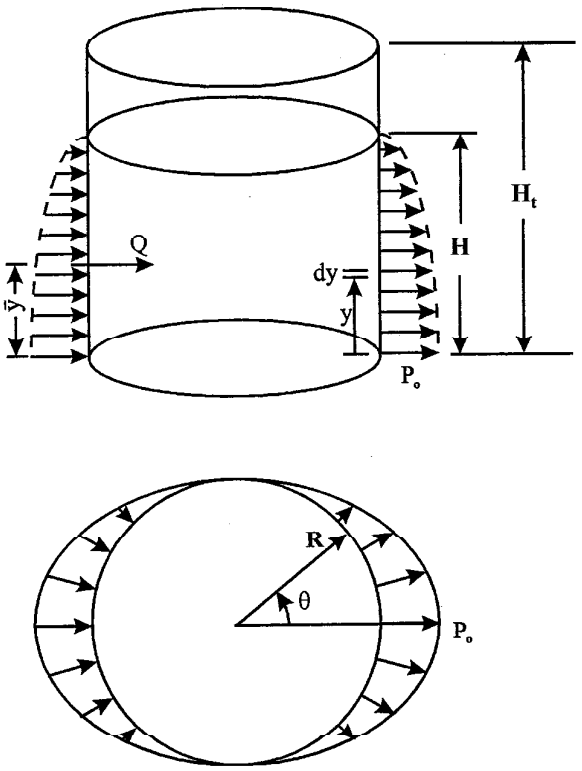

Figure 2: Pseudo-Dynamic Loads on Tank Wall

If M denotes the overturning moment about the center of the base, then

$$\begin{aligned} M &= \int_0^H \int_0^{2\pi} pRy\cos\theta\, d\theta\, dy = \frac{\pi}{4}H^2 p_o R \\ &= 278.3 p_o \end{aligned}$$

and similarly, if Q is the base shear, then

$$\begin{aligned} Q &= \int_0^H \int_0^{2\pi} pR\cos\theta\, d\theta\, dy - \frac{2\pi}{3}Hp_oR \\ &= 88.13 p_o \end{aligned}$$

and accordingly

$$\bar{y} = \frac{M}{Q} = 0.375H$$

In order to find the relationship between the seismic coefficient, c_1 (% of g), and the base pressure amplitude, p_o, the lateral seismic force from the assumed hydrodynamic pressure distribution is compared to the horizontal seismic force, thus

$$\begin{aligned} Q = \frac{2\pi}{3}Hp_oR &= c_1 W_f \\ &= c_1 \pi R^2 H \gamma_w \end{aligned}$$

where W_f is the weight of the fluid. Hence, one obtains,

$$p_o = \frac{3}{2}\gamma_w R c_1 = 702 c_1$$

4.1 Rigid-Tank Analysis

Assuming that the tank is completely rigid, the stability of the tank against overturning was evaluated. This analysis yielded a limiting value of the base pressure p_o at which the tank would overturn. Comparing the overturning moment with the stabilizing moment (see Figure (3)) gives

$$\text{Factor of Safety} = \frac{(W_w + W_r + W_f)R}{c_1 H(0.375 W_f) + c_1 H_t(0.5 W_w + W_r)}$$

where

W_f = weight of fluid = $\gamma_w \pi R^2 H$ = 61898 lb;
W_w = weight of tank shell = $\gamma_s 2\pi R t_w H_t$ = 6371 lb; and
W_r = weight of roof, base and equipment = 30000 − 6371 = 23629 lb (Note that the total weight = 30,000 lb).

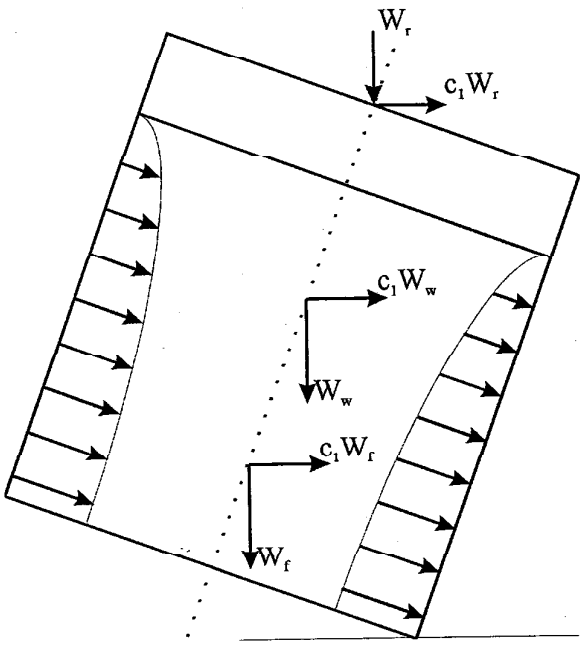

Figure 3: Stability of the Tank against Overturning

$$\text{Factor of Safety} = \frac{(91898)5}{c_1(8.42)(23212) + c_1(10.02)(3186 + 23629)}$$
$$\approx \frac{1.0}{c_1}$$

Hence, with a factor of safety of 1.0,

$$(c_1)_{\text{critical}} = 1.0$$

and the corresponding pressure amplitude,

$$(p_o)_{\text{critical}} = 702\,\text{lb/ft}^2$$

If only the fluid weight is considered in the stabilizing and overturning moments, then,

$$\text{Factor of Safety} = \frac{W_f R}{c_1 H(0.375 W_f)} = \frac{1.58}{c_1}$$

and accordingly, with a factor of safety of 1.0,

$$(c_1)_{\text{critical}} = 1.58$$

and the corresponding pressure amplitude,

$$(p_o)_{\text{critical}} = 1110\,\text{lb/ft}^2$$

4.2 Flexible-Tank Analysis (Small and Large Deflection)

Two finite element programs, DYNAZ and a commercial FEA package, were used to investigate the nonlinear static uplift of the tank under pseudo-dynamic loads. As shown in Figure (4), the DYNAZ model used 555 isoparametric shell elements with a total of 644 nodes; the tank rests on a flexible foundation. The stiffness of the floor was modeled in DYNAZ in two different ways: a uniform stiffness of 100 lb/in/in^2, or a variable stiffness according to a predefined function obtained by modeling the actual floor. A model using 231 beam elements and 451 shell elements was used as shown in Figure (5). The model was statically loaded with the weight of the MFH tank. The displacements obtained at the nodes were then curve fitted to a polynomial function, then used to obtain the equivalent spatial distribution of stiffness of the foundation springs. The displacement surface used is shown in Figure (6).

The second model for the commercial FEA program used 1128 shell elements with a total of 1130 nodes and it rests on a rigid surface, as shown in Figure (7).

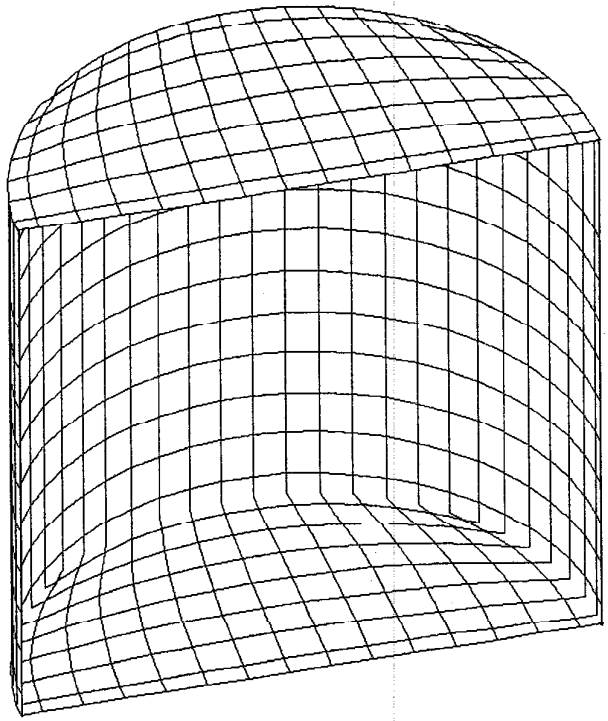

Figure 4: Finite Element Mesh of the MFH Tank for DYNAZ

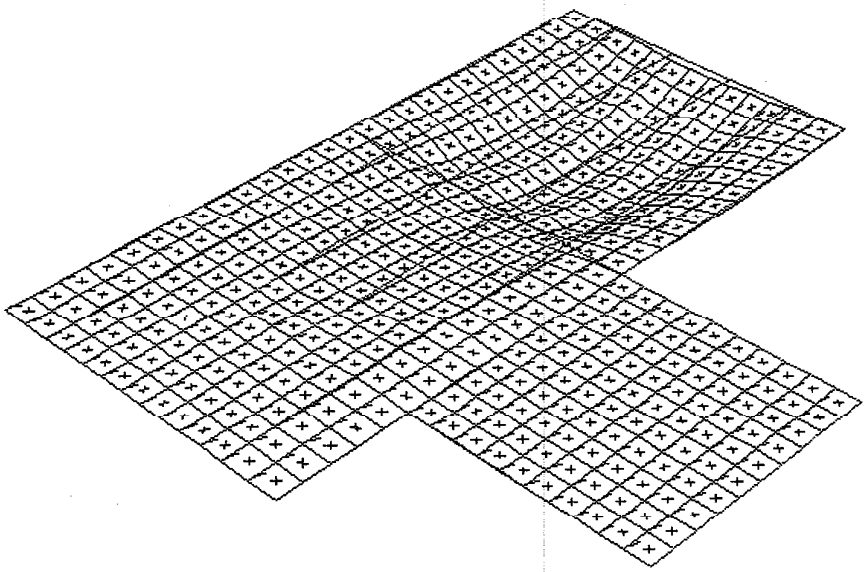

Figure 5: Deformed Shape of the Floor.

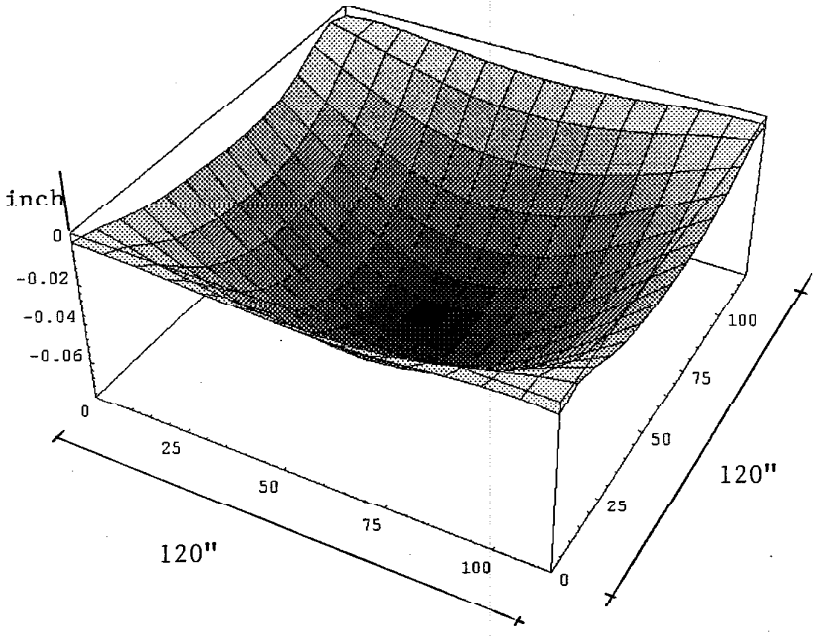

Figure 6: Displacement Surface used to Compute Foundation Stiffness

The two models were loaded up to the point of instability using various support conditions and deformation assumptions. Figure (7) shows the upward nodal displacements of the tank resting on a rigid surface just before the model became unstable. Figures (8) and (9) show the results of small and large deflection assumptions, respectively, considering the DYNAZ uniform floor stiffness model.

The two models produced consistent overturning moment values; they both compared well with the simple analytical rigid tank model (see section 4.1). This indicates that the shell of the MFH tank is very stiff and essentially the behavior can be likened to that of a rigid tank. In addition, it should be pointed out that considering large deflection and large rotation effects, the analysis indicated that the tank would overturn before it shows signs of buckling. Thus, plasticity and large deflection effect are ignored in subsequent dynamic analysis.

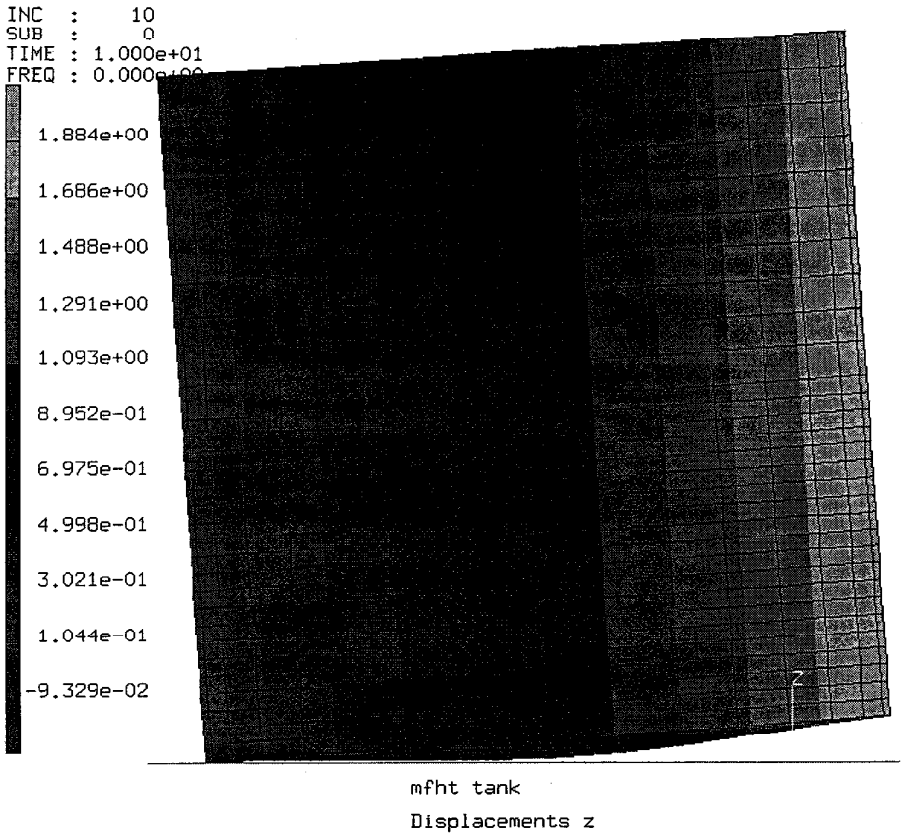

Figure 7: Upward Nodal Displacements of Tank just before Instability

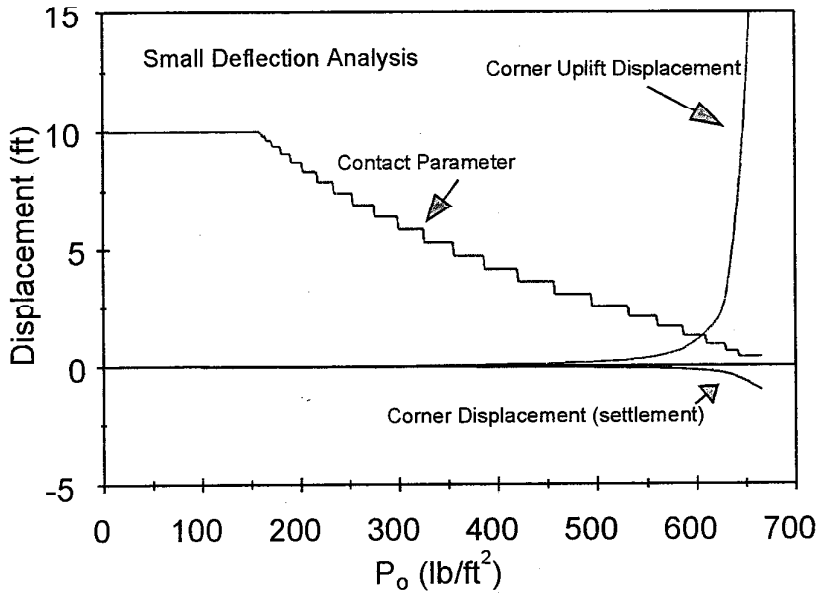

Figure 8: Static Small Deflection Analysis

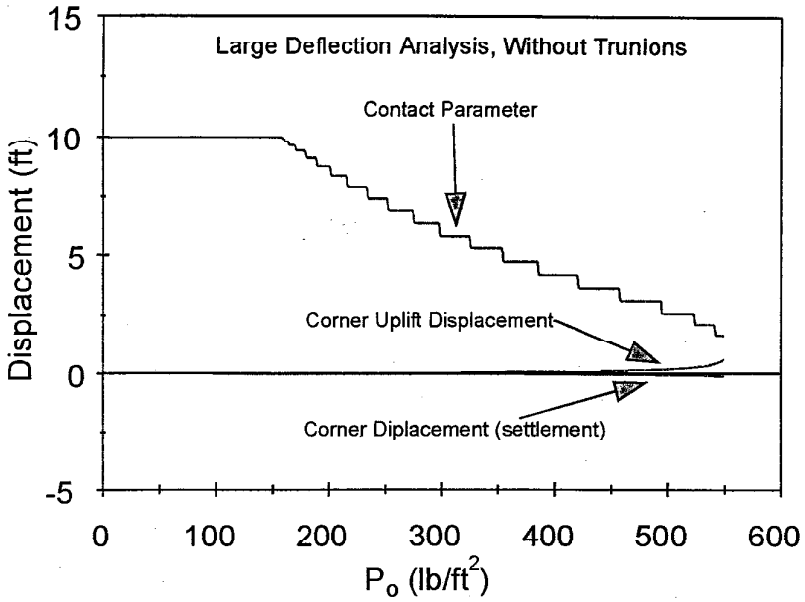

Figure 9: Static Large Deflection Analysis

5 Dynamic Analysis

In this phase, time history responses of the tank to different combinations of ground motions were evaluated. The ground motions used consisted of three earthquake component records labeled UX, UY and UV (Figure (10)). The three records were supplied by Dames & Moore and are the results of a SASSI analysis. They were obtained from node no. 1 of the SASSI model for the upper bound soil condition.

The effect of the fluid inside the tank was handled in two different approaches as follows:

5.1 Smeared Fluid Mass Model

In this model, 80% of the fluid mass (approximately corresponding to the impulsive mass) was smeared onto the shell using a parabolic distribution along the height of the tank and $|\cos\theta|$ distribution along the circumference of the tank. The remaining 20% of the fluid mass was equally smeared onto the base of the tank. Thus for the tank shell, the mass density, ρ, was distributed as

$$\rho = \rho_{\text{shell}} + \rho_o \left[1 - \left(\frac{y}{H}\right)^2\right] |\cos\theta|$$

where

$$\rho_o = 0.8 \times \rho_{\text{added-fluid}}$$

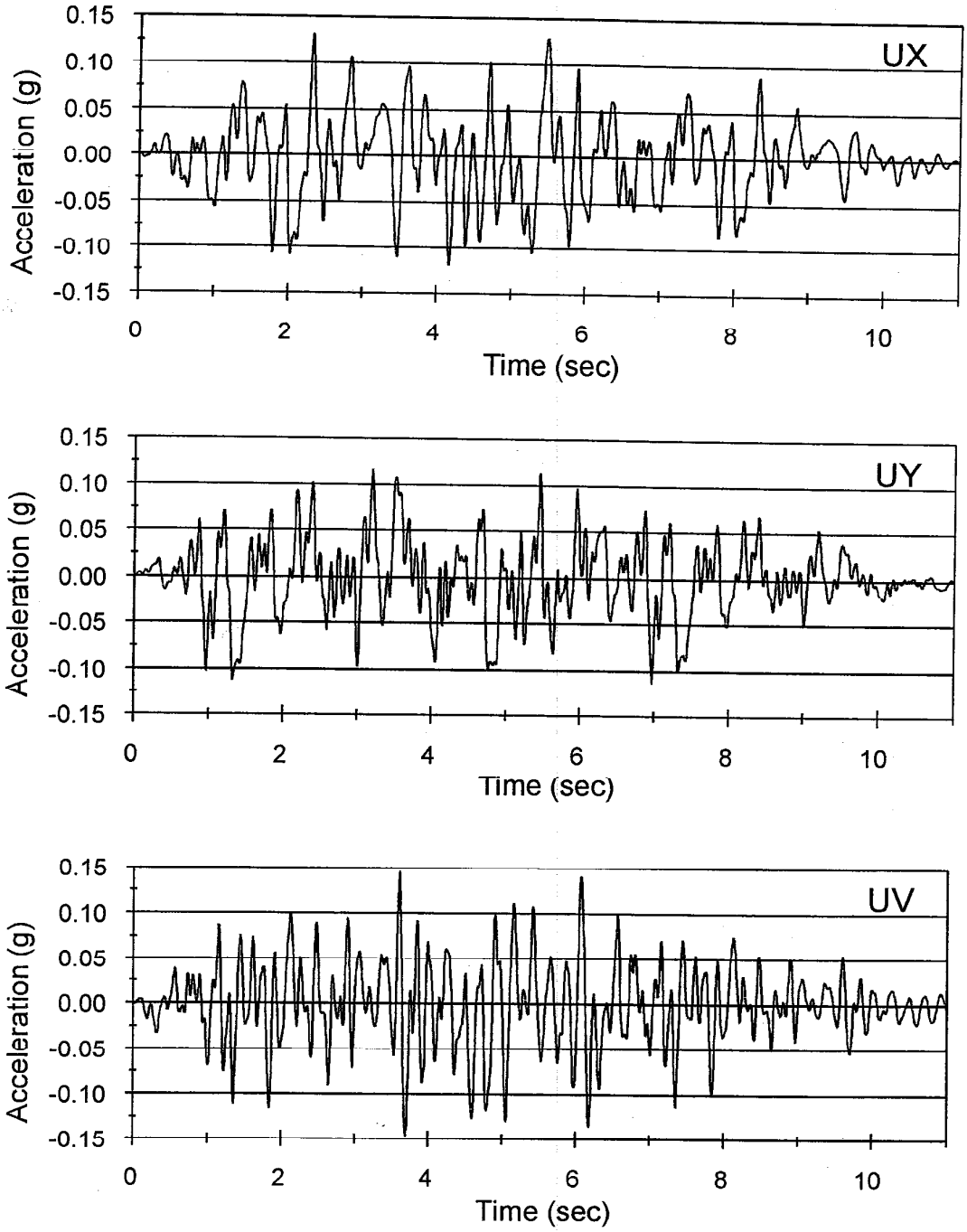

Figure 10: Earthquake Records

$$\rho_{\text{added-fluid}} = \frac{\pi R^2 \rho_f}{2\pi R t_w}$$
$$= \frac{R\rho_f}{2t_w} = 174.4 \text{ slug/ft}^3$$

For the tank base plate,

$$\rho = \rho_{\text{base}} + \rho_w \frac{H}{t_{\text{base}}}$$
$$= 406.7 \text{ slug/ft}^3$$

For the tank roof,

$$\rho = \frac{23629}{\pi R^2 g t_{\text{roof}}} = 128.2 \text{ slug/ft}^3$$

Table (1) shows the extreme values of the response to different scaling values of the horizontal earthquake component UX. All results were obtained using the program DYNAZ.

Component Label	UX	UX	UX
Scale factor	100%	200%	300%
Max. Uplift Displacement (in)	0.019	0.173	0.277
Max. Lateral Displacement (in)	0.095	0.331	0.478
Base Shear / W_f	0.151	0.285	0.403
OTM / $W_f R$	0.130	0.261	0.398
Minimum Contact Area Ratio	0.880	0.648	0.599

Table 1: Response to Horizontal Earthquake Component UX, 3% Foundation Damping (Smeared Mass Model)

5.2 Fully-Coupled Fluid-Structure Interaction with Free Surface Sloshing Model

In this model, the fluid in the tank was explicitly modeled using DYNAZ. The finite element formulation simulated both the fluid-structure interaction and the free surface sloshing.

As shown in Figure (11), the fluid inside the tank was discretized to 500 fluid elements with a total of 726 nodes. The tank was discretized to 359 isoparametric shell element with a total of 428 nodes. The response of the tank is governed primarily by the rocking mode. Fourier decomposition of the tank response showed that this mode has a dominant period of 0.3 sec. for the uniform floor stiffness model and 0.22 sec. for the variable floor stiffness model. Based on these periods, the foundation rocking damping is estimated. Summary of results of the variable floor stiffness model are presented for three different foundation

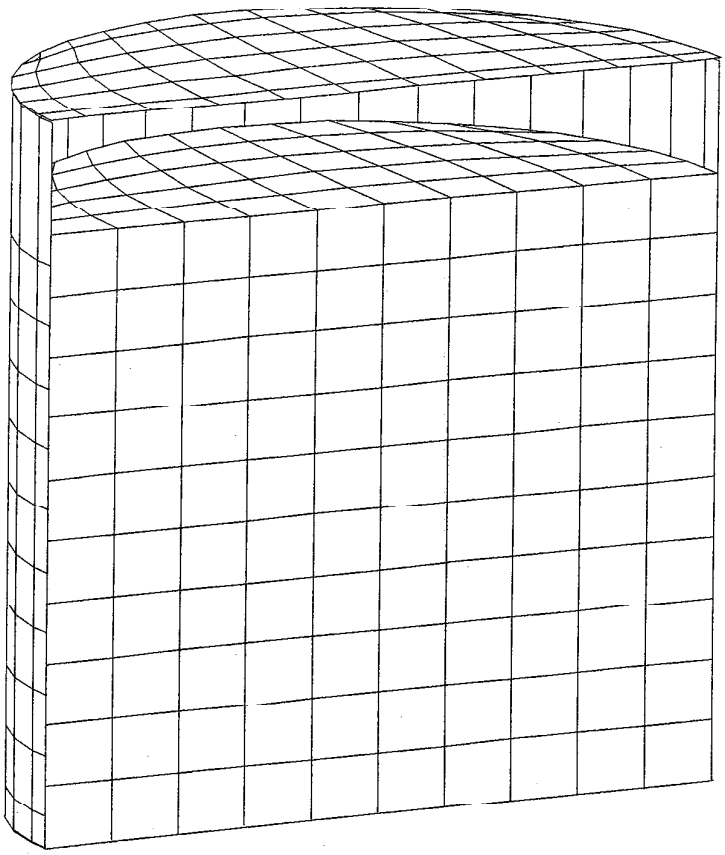

Figure 11: Finite Element Mesh of the Coupled Fluid-Tank System

Component Label	UX	UX	UX	UX	UX
Scale	100%	200%	300%	400%	500%
Max. Uplift Displacement (in)	0.026	0.141	0.384	0.761	1.068
Max. Lateral Displacement (in)	0.103	0.278	0.590	1.029	1.371
Base Shear / W_f	0.193	0.341	0.492	0.651	0.749
OTM / $W_f R$	0.139	0.247	0.339	0.487	0.551
Minimum Contact Area Ratio	0.817	0.671	0.524	0.427	0.366

Component Label	UX+UV	UX+UV	UY	UY+UV	UY+UV
Scale	300%	400%	400%	300%	400%
Max. Uplift Displacement (in)	0.543	0.859	0.204	0.179	0.608
Max. Lateral Displacement (in)	0.843	1.274	0.314	0.278	0.706
Base Shear / W_f	0.535	0.699	0.477	0.475	0.637
OTM / $W_f R$	0.611	0.820	0.355	0.390	0.578
Minimum Contact Area Ratio	0.488	0.427	0.598	0.585	0.390

Table 2: Extreme Values of Response, 3% Foundation Damping (Fully Coupled Model)

damping ratios: 3% (conservative) in Table (2), 10% (estimated typical) in Table (3) and 20% in Table (4). It was decided that the most critical (and reasonable) case is when the applied ground motion is scaled upward by 400% with 10% foundation damping. Results from a fully-coupled analysis are shown in Figure (12) to Figure (22).

Component Label	UX	UX	UX
Scale	300%	400%	500%
Max. Uplift Displacement (in)	0.262	0.450	0.623
Max. Lateral Displacement (in)	0.448	0.695	0.911
Base Shear / W_f	0.493	0.650	0.784
OTM / $W_f R$	0.341	0.456	0.544
Min. Contact Area Ratio	0.610	0.512	0.463

Component Label	UX+UV	UX+UV	UY	UY+UV	UY+UV
Scale	300%	400%	500%	300%	400%
Max. Uplift Displacement (in)	0.346	0.531	0.276	0.346	0.349
Max. Lateral Displacement (in)	0.579	0.851	0.401	0.579	0.462
Base Shear / W_f	0.464	0.608	0.581	0.464	0.637
OTM / $W_f R$	0.536	0.708	0.401	0.536	0.514
Min. Contact Area Ratio	0.573	0.524	0.561	0.573	0.463

Table 3: Extreme Values of Response, 10% Foundation Damping

Component Label	UX	UX	UX	UY
Scale	500%	600%	700%	600%
Max. Uplift Displacement (in)	0.426	0.634	0.887	0.287
Max. Lateral Displacement (in)	0.664	0.914	1.214	0.424
Base Shear / W_f	0.773	0.894	1.016	0.707
OTM / $W_f R$	0.531	0.620	0.714	0.486
Min. Contact Area Ratio	0.524	0.415	0.305	0.549

Table 4: Extreme Values of Response, 20% Foundation Damping

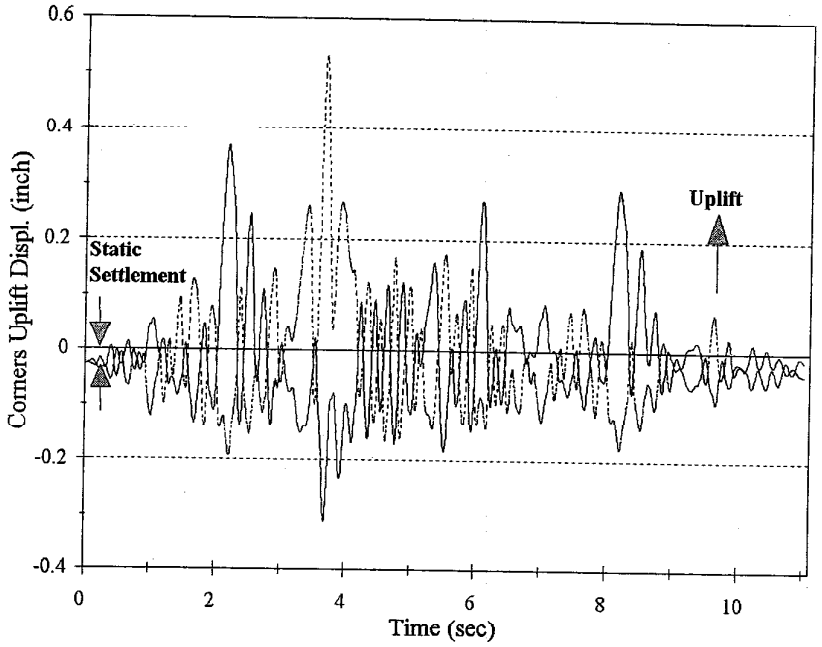

Figure 12: Uplift Displacement of the Two Extreme Bottom Corners* of MFH Tank using 400% (UX+UV) for 10% Foundation Damping
*Two points at the ends of the principal diameter that parallels the earthquake excitation

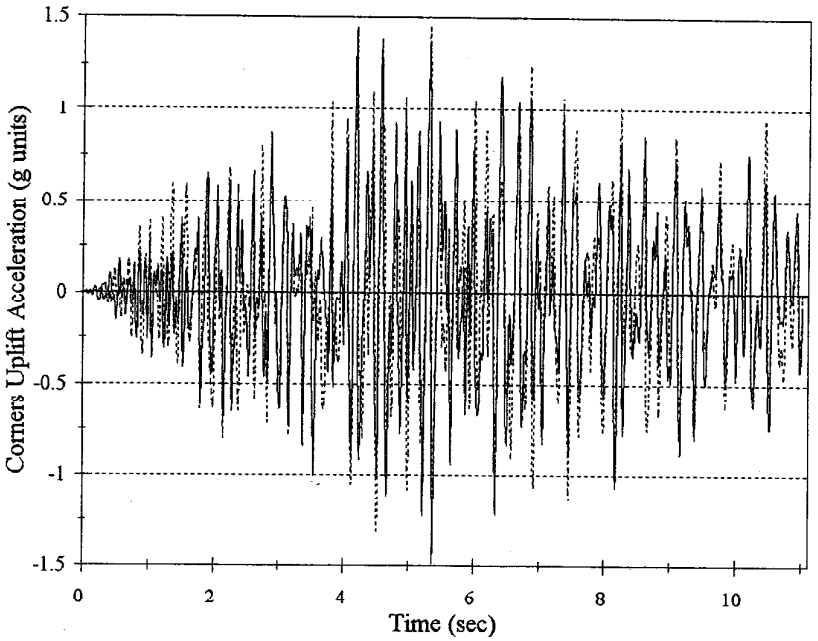

Figure 13: Vertical Acceleration of the Two Extreme Bottom Corners of MFH Tank using 400% (UX+UV) for 10% Foundation Damping

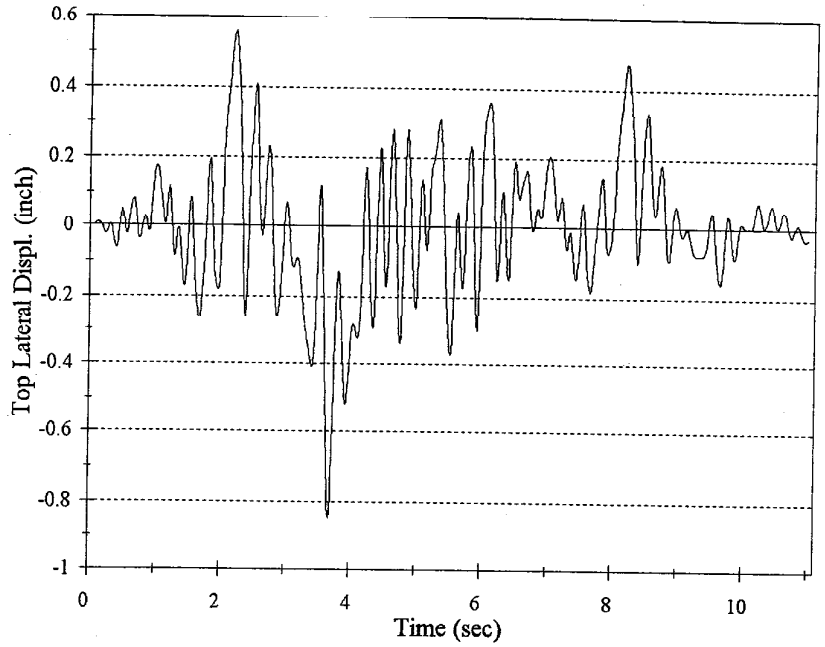

Figure 14: Lateral Displacement at Top of MFH Tank using 400% (UX+UV) for 10% Foundation Damping

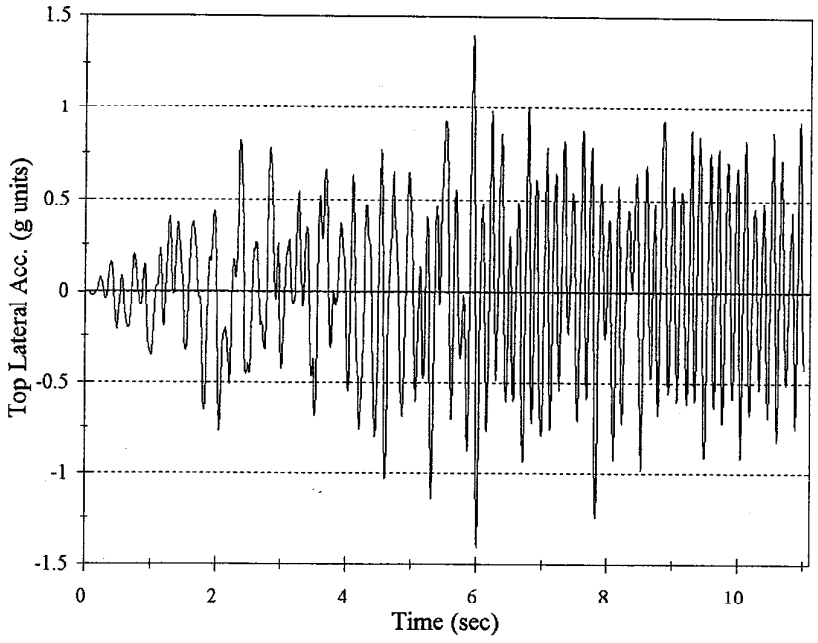

Figure 15: Lateral Acceleration at Top of MFH Tank using 400% (UX+UV) for 10% Foundation Damping

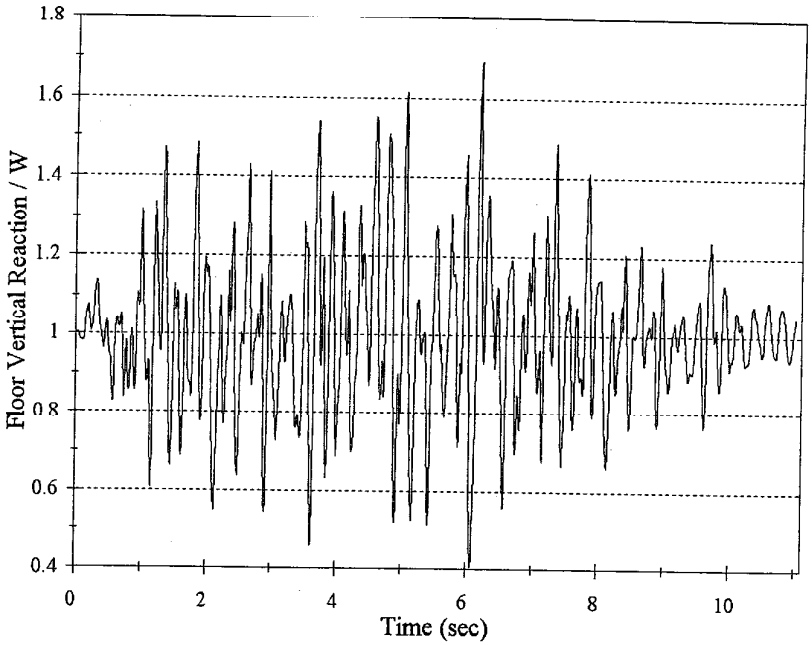

Figure 16: Total* Vertical Reaction of MFH Tank using 400% (UX+UV) for 10% Foundation Damping

* Integration of the floor pressure over the contact area

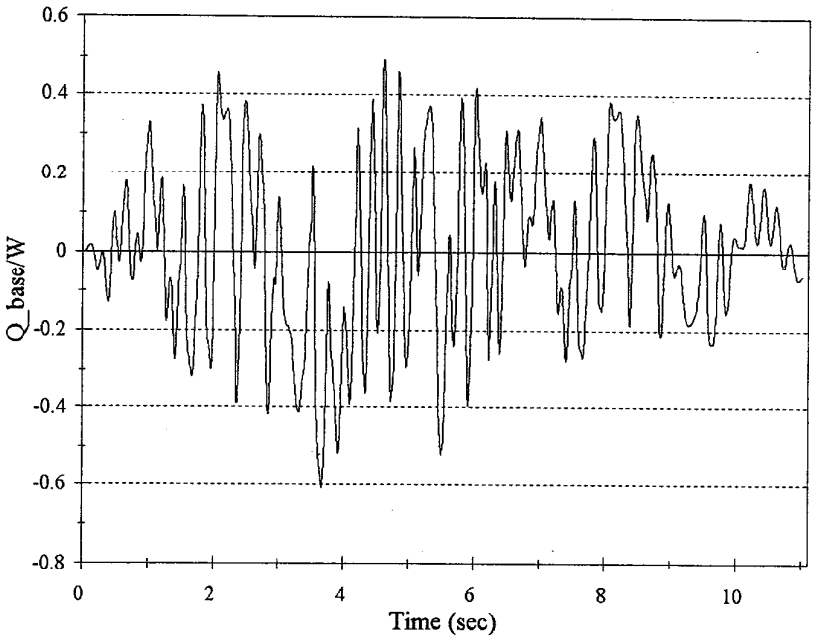

Figure 17: Base Shear of MFH Tank using 400% (UX+UV) for 10% Foundation Damping

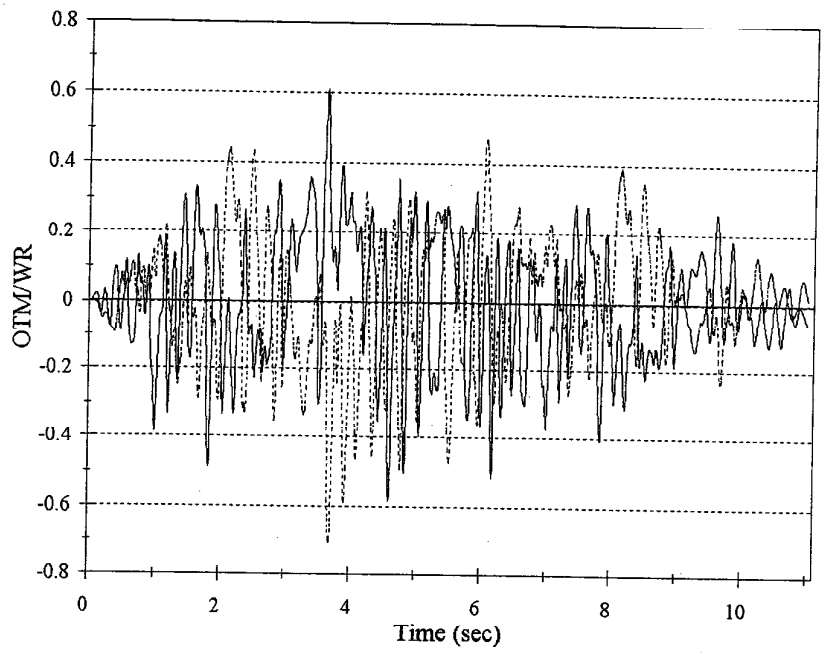

Figure 18: Overturning Moment about Center of the Base of MFH Tank using 400% (UX+UV) for 10% Foundation Damping

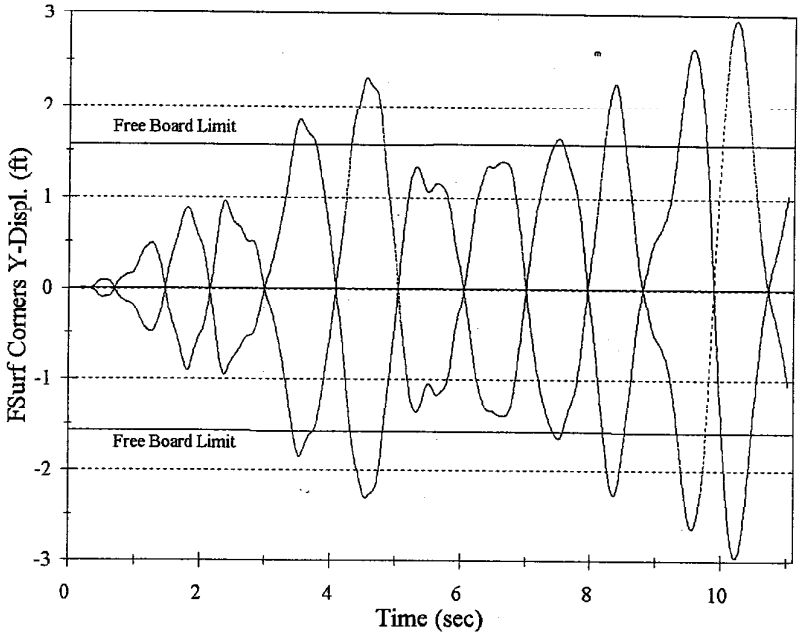

Figure 19: Sloshing Height of Fluid in MFH Tank using 400% (UX+UV) for 10% Foundation Damping

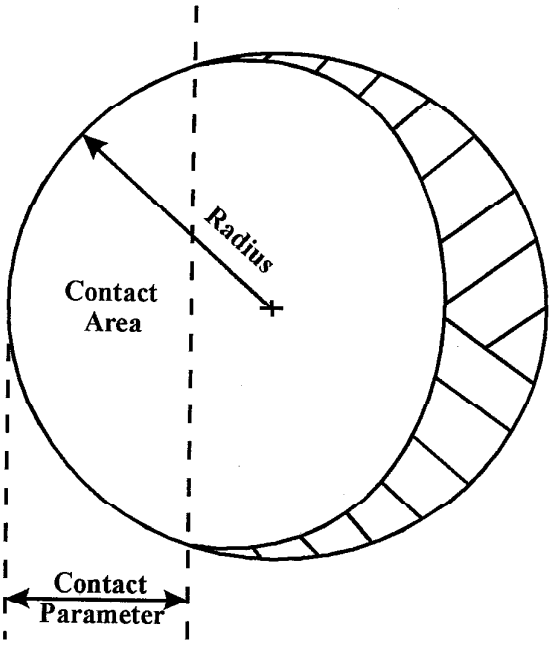

Figure 20: Definition of Contact Parameter

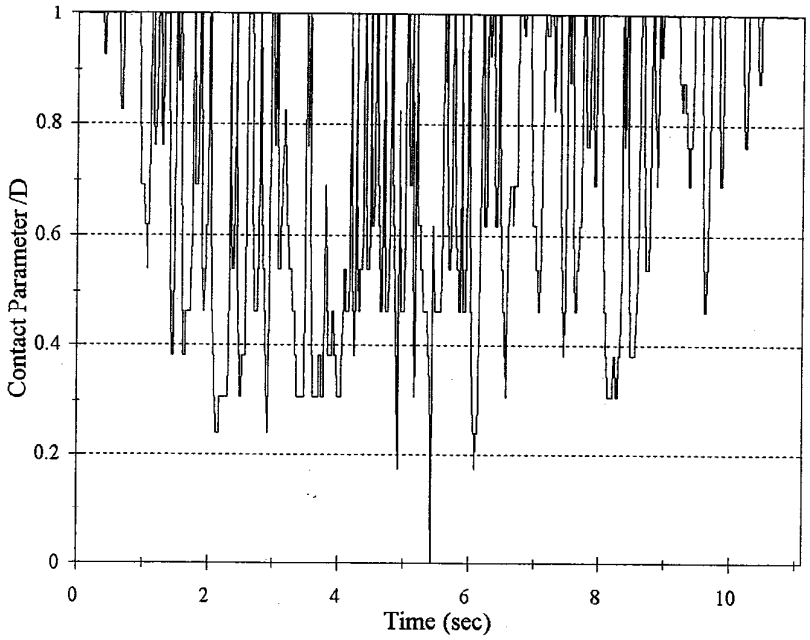

Figure 21: Contact Parameter of the Base of MFH Tank using 400% (UX+UV) for 10% Foundation Damping

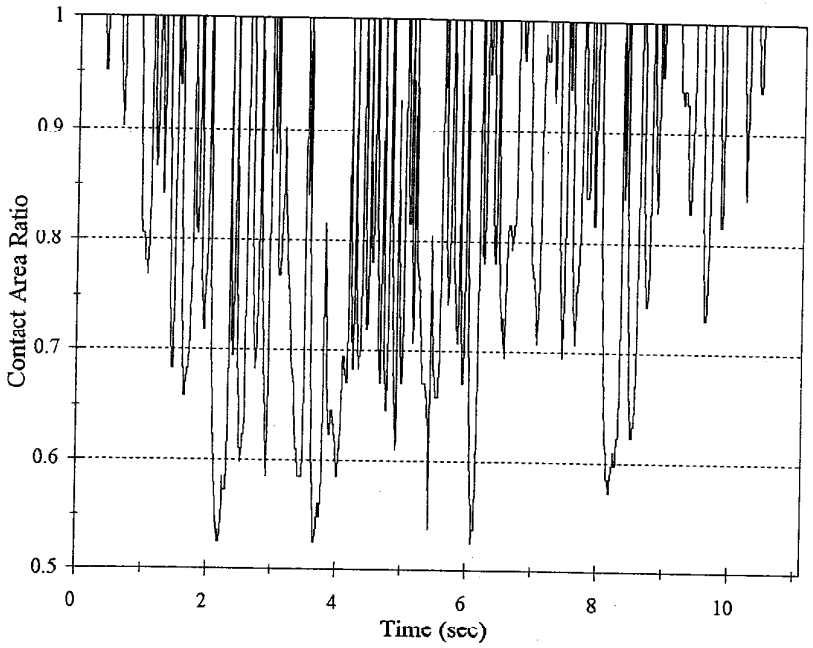

Figure 22: Fraction of Base Area in Contact with Foundation in MFH Tank using 400% (UX+UV) for 10% Foundation Damping

6 Summary of Computer Runs

The following runs were performed in order to evaluate the seismic capacity of the MFH tank:

1. Static analysis using both small and large deflection assumptions on both DYNAZ and a commercial finite element software
2. Dynamic analysis of the smeared fluid mass model using DYNAZ
3. Dynamic analysis of the fully coupled fluid-structure interaction model using DYNAZ

7 Conclusion

Based on the performed analyses summarized in Section 6, it is expected that the tank would safely resist overturning and buckling under earthquake motion at a higher level than that supplied by the SASSI analysis.

REFERENCES

[1] Kock, E., and Olson, L., *Fluid Structure Interaction Analysis by the Finite Element Method - a Variational Approach*, International Journal for Numerical Methods in Engineering, Vol. 31, No. 3, March, 1991, pp. 463-491.

[2] El-Zeiny, A., *Nonlinear Time-Dependent Seismic Response of Unanchored Liquid Storage Tanks*, Ph.D. Dissertation, Department of Civil and Environmental Engineering, University of California, Irvine, 1995.

[3] Haroun, M.A., and Zeiny, A., *Nonlinear Transient Response of Unanchored Liquid Storage Tanks*, Proceedings of the Pressure Vessels and Piping Conference, ASME, Vol. 314, Hawaii, July 1995, pp. 35-41.

[4] Haroun, M.A., and Zeiny, A., *Simulation of Dynamic Behavior of Unanchored Tanks*, Proceedings of the 13th International Conference on Structural Mechanics in Reactor Technology (SMIRT-13), Porto Alegre, Brazil, August 1995.

[5] Haroun, M.A., and Housner, G.W., *Dynamic Characteristics of Liquid Storage Tanks*, Journal of Engineering mechanics, Div. ASCE, Vol. 108, 1982, pp. 783-800.

[6] Haroun, M.A., *Earthquake Response of Deformable Liquid Storage Tanks*, Journal of Applied Mechanics, ASME, Vol. 48, No. 2, June, 1981, pp. 411-418.

[7] Hughes, T.J.R., and Liu, W.K. *Nonlinear Finite Element Analysis of Shells: Part I. Three-Dimensional Shells*, Journal of Computer Methods in Applied Mechanics and Engineering, Vol. 26, 1981, pp. 331-362.

[8] Olson, L., and Bathe, K.J., *An Infinite Element for Analysis of Transient Fluid-Structure Interaction*, Journal of Engineering Computation, December, 1985, Vol. 2, pp. 319-329.

[9] Lamb, H., *Hydrodynamics*, 6th Edition, Dover Publications, New York, 1945.